ACS APPLIED MATERIALS & INTERFACES

Research Article

www.acsami.org

Pressure-Sensitive Adhesion System Using Acrylate Block Copolymers in Response to Photoirradiation and Postbaking as the Dual External Stimuli for On-Demand Dismantling

Tadashi Inui, Eriko Sato,* and Akikazu Matsumoto*

Department of Applied Chemistry and Bioengineering, Graduate School of Engineering, Osaka City University, 3-3-138, Sugimoto, Sumiyoshi-ku, Osaka 558-8585, Japan

Supporting Information

ABSTRACT: We have demonstrated the validity of a new type of pressure-sensitive adhesion system using block copolymers containing a poly(2-ethylhexyl acrylate) (P2EHA) segment as the low glass transition temperature polymer and a poly(*tert*-butyl acrylate) (PtBA) or poly(isobornyl acrylate) (PIBoA) segment as the reacting polymer in the presence of a photoacid generator (PAG). This adhesion system can be easily debonded because of a change in the polymer properties of the adhesives by acid-catalyzed deprotection uniquely occurring during the photoirradiation followed by postbaking. We investigated the transformation of PtBA and PIBoA into poly(acrylic acid) using IR spectroscopy and a thermogravimetric analysis in the presence of *p*-toluenesulfonic acid and the PAGs. The block copolymers with a well-defined molecular structure were then synthesized by atom transfer radical polymerization, and their adhesive properties were evaluated using the 180° peel test. The block copolymers showed superior adhesion property than a random copolymer and polymer blends, due to the microphase separation of the block copolymers. A drastic change in the adhesive strength of the block copolymers was observed in response to the dual external stimuli consisting of UV irradiation and the subsequent heating.

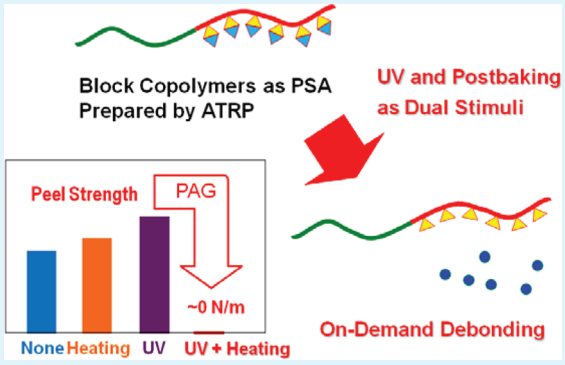

KEYWORDS: *pressure-sensitive adhesive, living radical polymerization, dismantlable adhesion, block copolymer, photoacid generator, acrylic polymer*

INTRODUCTION

Acrylic polymers with a low glass transition temperature are used as pressure-sensitive adhesives in various application fields, such as electronics, automobiles, office automation, packing, and daily necessities.[1] High-strength pressure-sensitive adhesives are often used when a high-strength and long-term adhesion is required, but the debonding process becomes more difficult at the same time. Recently, dismantlable adhesion, a new kind of on-demand dismounting technology and materials, has attracted attention because of saving materials and energy.[2−9] For dismantlable adhesive materials, their adhesive property instantaneously changes in response to any external stimulus as the trigger for dismantling, for example, heating,[10−14] UV irradiation,[15] induction heating,[16] electricity,[17] and chemicals.[18] A change in the physical properties of adhesives is important for dismantling in many cases, but chemical reactions are expected to sharply change the polymer properties.[15,18] In a previous paper,[19] we reported a dismantlable adhesion system using linear and network polyperoxides, which contain peroxy bonds in the main-chain repeating units or at the cross-linking points. The degradation of the polyperoxides rapidly occurs via a radical chain reaction mechanism,[20−23] resulting in a significant change in their molecular weight and physical properties. The dismantlable adhesion using the polyperoxides is responsive to heat or UV irradiation and leads to a drastic change in the adhesion properties, but the polyperoxide adhesion system has some problems for use in certain application fields, for example, thermal stability, long pot-life, and safety during handling. Easy debonding is inconsistent with the adhesive properties in order to guarantee the quality and safety of the products during use.

We now propose a dual-locked type of adhesion system, requiring two different kinds of triggers for dismounting, in order to avoid the trade-off relationship of stability during use and high sensitivity to stimuli upon dismantling. In this system, the adhesive polymers with a protected functional group are stable during use even when a single external stimulus of either UV irradiation or heating is applied, but their properties quickly change in response to UV irradiation and postbaking as the dual stimuli. We have determined the adhesive properties of the acrylate polymers during which the side chain is transformed into a carboxylic acid upon heating by acid-catalyzed

Received: January 18, 2012
Accepted: March 19, 2012
Published: March 19, 2012

deprotection, and demonstrated the validity of the dual-locked adhesion system using a block copolymer as the pressure-sensitive adhesive in the presence of a photoacid generator (PAG). The transformation of some protected functional groups into the corresponding unprotected groups using PAGs is widely used in a chemically amplified photoresist process, which was first proposed by Ito and co-workers in 1982.[24,25] This process includes a large number of repeated chemical transformations induced by a single photochemical event in the photoresist polymers, resulting in a highly efficient polymer reaction. It consists of photoirradiation producing a small amount of active species (proton) for chemical reactions and the subsequent heating of the exposed resist materials (postbaking) for the diffusion of the protons and the occurrence of many reaction cycles.

In this study, we investigated the thermal decomposition behavior of poly(*tert*-butyl acrylate) (PtBA) and poly(isobornyl acrylate) (PIBoA) in the presence of *p*-toluenesulfonic acid (TsOH) as the acid or bis(cyclohexylsulfonyl)diazomethane (BCD) and *N*-trifluoromethylsulfonyloxy-1,8-naphthalimide (NIT) as the PAGs to produce poly(acrylic acid) (PAA) with the evolution of isobutene[26−28] and camphene[29−31] from PtBA and PIBoA, respectively (Scheme 1). PtBA and PIBoA were

Scheme 1

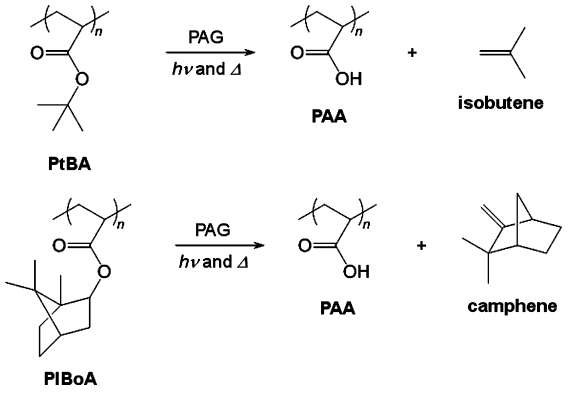

used as the adhesive polymer materials in combination with poly(2-ethylhexyl acrylate) (P2EHA) with a low glass transition temperature (T_g). The block copolymers consisting of P2EHA as the low-T_g polymer segment and PtBA or PIBoA as the reactive polymer segment with a well-controlled structure, such as the molecular weight, molecular weight distribution, and composition, were then synthesized by atom transfer radical polymerization (ATRP), and their adhesion properties were investigated in the presence of the acid and the PAGs.

EXPERIMENTAL SECTION

General Procedure. The NMR spectra were recorded using a Bruker AV300 spectrometer in chloroform-*d* or acetone-d_6 as the solvents. The FT-IR spectra were recorded using a JASCO FT/IR 430 spectrometer. The number- and weight-average molecular weights (M_n and M_w) were determined by size exclusion chromatography (SEC) in tetrahydrofuran (THF) as the eluent using a Tosoh CCPD RE-8020 system and calibration with standard polystyrenes. The thermogravimetric and differential thermal analyses (TG/DTA) were performed using a Seiko TG/DTA6200 at the heating rate of 10 °C/min in a nitrogen stream at the flow rate of 200 mL/min. The differential scanning calorimetric (DSC) analysis was performed using a Seiko EXSTAR6200 at the heating rate of 10 °C/min. Atomic force microscope (AFM) images were observed using a NanoScope IIIa system (Digital Instruments/Veeco) with a cantilever (OMCL-AC240TS-C2, Olympus, spring constant 2 N/m, resonant frequency 70 kHz) in height and phase modes. The samples for AFM measurement were prepared on a paper on which the adhesive polymer with and without PAG in acetone was coated and dried overnight under reduced pressure at room temperature.

Materials. The acrylate monomers, *tert*-butyl, 2-ethylhexyl, isobornyl, and cyclohexyl acrylates (tBA, 2EHA, IBoA, and CHA, respectively) were purchased from Tokyo Chemical Industry Corporation, Ltd., and distilled before use. Bornyl acrylate (BoA) was synthesized from acryloyl chloride and (−)-borneol. The commercially available TsOH (99.0%, Wako Pure Chemical Industries Corporation, Ltd.), BCD (98.0%, Wako Pure Chemical Industries Corporation, Ltd.,), NIT (99%, Sigma-Aldrich Co.), CuBr (99.9%, Wako Pure Chemical Industries Corporation, Ltd.), methyl 2-bromopropionate (MBP) (97.0%, Tokyo Chemical Industry Corporation, Ltd.), and dimethyl 2,6-dibromohenptanoate (BDH) (97%, Sigma-Aldrich Co.) were used as received. All the solvents were distilled before use. Tris(2-(dimethylamino)ethyl)amine (Me_6TREN) was synthesized according to a method described in the literature.[32]

Polymerization. Typical procedures for the polymerization are as follows.[33] In a 50 mL Schlenk flask, tBA (9.0 g, 70 mmol), Me_6TREN (0.078 mL, 0.29 mmol), 7.4 mL of toluene, and 3.5 mL of acetone were charged, and the solution was degassed by a freeze−thaw technique (three times), then the argon was purged. After CuBr (42.0 mg, 0.29 mmol) was added and stirred for 15 min at room temperature, MBP (0.13 mL, 1.2 mmol) was added. After the polymerization at 60 °C for 1 h, an aliquot was analyzed by ^{1}H NMR spectroscopy and SEC in order to determine the conversion, molecular weight, and its distribution. The polymerization mixture was passed through a short silica gel column with acetone in order to remove the catalyst, and then the acetone and the unreacted monomer were removed under reduced pressure at 40 °C for 12 h. The $M_{n,SEC}$ and M_w/M_n values of the isolated PtBA were 4400 and 1.13, respectively. The conversion was 50.1%. The functionality of the ω-chain end was 0.98.

In order to obtain a block copolymer, the PtBA macroinitiator (0.78 g), 2EHA (3.57 g, 19.4 mmol), Me_6TREN (0.026 mL, 0.096 mmol), and 1.45 g of ethyl acetate were charged, then the solution was degassed by a freeze−thaw technique (three times), followed by argon purging. After CuBr (13.9 mg, 0.097 mmol) was added and stirred, the polymerization was carried out at 60 °C for 25 min. The conversion of 2EHA was 93.8%. The polymerization mixture was passed through a short silica gel column with acetone in order to remove the catalyst. The recovered solution was concentrated and poured into a mixture of methanol and water (80/20 in volume ratio), the block copolymer was isolated by decantation, and then dried under reduced pressure at 40 °C for 12 h. The $M_{n,SEC}$ and M_w/M_n values of the isolated PtBA-*block*-P2EHA were 18 600 and 1.23, respectively. The degrees of polymerization (*DP*) were 30 and 95 for the PtBA and P2EHA segments, respectively.

Other macroinitiators and block copolymers were similarly synthesized.

Adhesion Test. The adhesion tests were performed according to the standard test method for the peel adhesion of pressure-sensitive tape (ASTM D3330) using a Tokyo Testing Machine (TTM) universal testing machine, LSC-1/30, with a 1 kN (at maximum) load cell. The adhesive polymers (30 wt %) with or without a determined amount of PAG or TsOH in toluene or acetone were coated with a thickness of 100 μm on a poly(ethylene terephthalate) (PET) film (50 μm thickness) using a film applicator, and dried overnight under reduced pressure at room temperature. The thickness of the adhesive layer was approximately 30 μm after drying. A strip of the PET film (2-cm width) coated with the adhesive polymers was placed to a stainless steel plate (SUS430, 50 mm × 150 mm × 0.5 mm), and then pressed using a 2-kg hand roller. The UV irradiation, heating, and 180° peel test were carried out after the specimen was left to stand over 30 min at room temperature. For the UV irradiation, the test piece was placed at a distance of 10 cm from the UV source (Toshiba SHL-100UVQ-2) at room temperature. For the thermal treatment, the test piece was

placed in a preheated oven for a predetermined time, removed from the oven, and then naturally cooled to room temperature. All the adhesion tests were performed at 23 °C. The average value of three measurements was typically recorded.

RESULTS AND DISCUSSION

Acid-Catalyzed Deprotection of PtBA. The elimination of isobutene from the side chain of PtBA to produce PAA in the presence of TsOH as the acidic catalyst was investigated by IR spectroscopy and a TG analysis. The PtBA films containing 5 mol % of TsOH versus the *tert*-butyl group were heated at various temperatures for 10 min or 1 h (Figure 1). After heating, the intensity of the peaks due to the C−H deformation of the methyl group at 1392 and 1367 cm^{-1}, the C−O stretching of the *tert*-butoxyl group at 1150 and 1256 cm^{-1}, and the O−C−C out-of-plane deformation of the same group at 846 cm^{-1} decreased and a broad peak due to a carboxylic acid appeared around 3000 cm^{-1}. At the same time, the peak due to the carbonyl stretching at 1729 cm^{-1} shifted to 1710 cm^{-1}. The heating at 120 °C for 10 min or 100 °C for 1 h resulted in the PAA formation at a high conversion (>95%). On the other hand, no change was seen in the spectrum after heating at 150 °C for 1 h in the absence of TsOH. It was also confirmed that when the PtBA was heated at 200 °C, the acid anhydride was produced based on the appearance of the peaks at 1802 and 1757 cm^{-1}. This indicated that PtBA is thermally stable even at 150 °C, while the reaction is drastically accelerated by the addition of the acid.

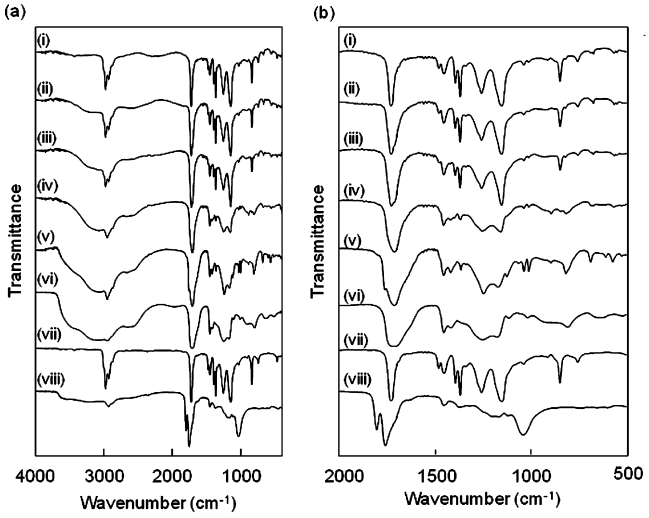

Figure 1. (a) IR spectra of PtBA films containing 5 mol % TsOH versus the *tert*-butyl group (i) before and (ii−v) after heating at (ii) 80, (iii) 100, and (iv) 120 °C for 10 min, and (v) 100 °C for 1 h (7 mol % TsOH). (vi) Commercial PAA as the film, after heating at (vii) 150 and (viii) 200 °C for 1 h in the absence of TsOH. (b) Expanded.

The amount of isobutene evolved from the side chain of PtBA during the deprotection was determined by a TG analysis. Figure 2 shows the TG curves of PtBA in the presence of various amounts of TsOH. The onset temperature of the isobutene elimination, i.e., the 5 wt % weight-loss temperature (T_{d5}), the maximum decomposition temperature (T_{max}), the end-point temperature of the first-step decomposition (T_{end}), and the weight-loss values (X) for the olefin elimination during the first-step reaction accompanying a rapid weight-loss are determined and summarized in Table S1 (see the Supporting Information). The T_{d5} value for PtBA decreased from 171 °C (0.1 mol % of TsOH) to 82 °C (6.0 mol % of TsOH) according to the amount of added TsOH. When PtBA contains no TsOH, the weight loss started over 200 °C (T_{d5} = 232.7 °C and T_{max} = 235.0 °C) and the weight-loss value was 46.3% at 246.5 °C after the rapid olefin elimination. The magnitude of the weight loss was greater than the theoretical value (43.8%) for the quantitative elimination of isobutene from PtBA. At a temperature over 200 °C, dehydration further occurs between the carboxylic acid moieties to produce the acid anhydride via intra- and intermolecular reactions (see also Figure 1). In Figure 2a, the TG traces in a temperature range higher than 280 °C were the same, in contrast to a drastic change in the isobutene elimination behavior depending on the added TsOH amount. The observed weight-loss value (51.7% at 280 °C) was higher than the theoretical weight-loss value (50.8%) for the complete anhydride formation due to the occurrence of other decompositions.

The acid-catalyzed deprotection of the *tert*-butyl ester group of PtBA occurs via a diffusion-controlled reaction mechanism and the reaction behavior significantly depends on the T_g of the polymers. The T_g value of PtBA was 39 °C, which was slightly

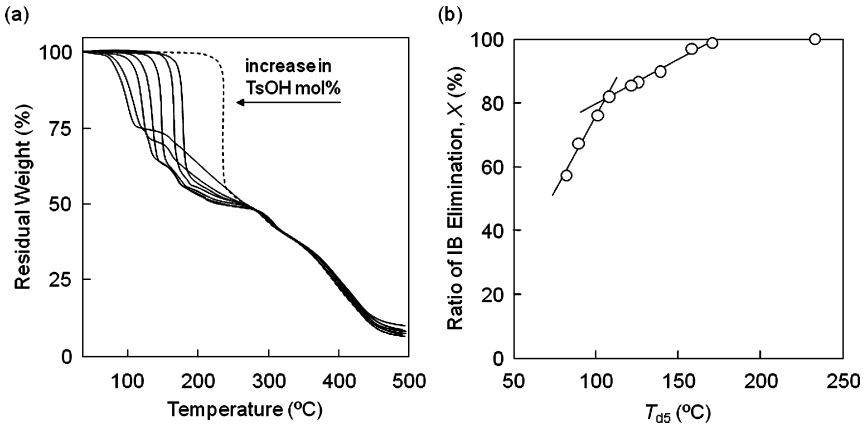

Figure 2. (a) TG curves for PtBA in the presence of TsOH (0.1, 0.2, 0.5, 1.0, 1.5, 4.0, and 6.0 mol % versus the *tert*-butyl group) (solid curves) and in the absence of TsOH (dash curve) at the heating rate of 10 °C/min in a nitrogen stream. (b) Relationship between the T_{d5} value and the ratio of isobutene elimination (X) during the first-step decomposition evaluated based on the magnitude of the rapid weight-loss during the first-step reaction process in the TG curves.

dx.doi.org/10.1021/am300103c | ACS Appl. Mater. Interfaces 2012, 4, 2124−2132

lower than the value (55 °C) reported in the literature[34] due to difference in the molecular weight. A readily mobile proton effectively functions as the chemically amplifying catalyst in the polymer in a temperature range over the T_g, but the reaction is suppressed at the glassy state below the T_g. In this study, therefore, the X value was drastically reduced (Figure 2b) when the T_{d5} was lower than the T_g of the PAA, which was reported to be 103 °C.[35,36] The temperature and magnitude of the rapid weight-loss due to the isobutene elimination depended on the TsOH amount as was already described. The slope of the weight-loss curve was very high in the absence of TsOH, while an increase in the amount of the added TsOH resulted in the broader TG curves due to the suppression of the reaction as shown in Figure 2a.

Acid-Catalyzed Deprotection of PIBoA. The thermal and acid-catalyzed deprotection behaviors of polyacrylates with a secondary alkyl ester group were also investigated. The TG curves for PIBoA and PBoA in the absence and presence of TsOH are shown in Figure 3 (see also Figure S1 in the Supporting Information). The thermal decomposition (i.e., olefin elimination) of PIBoA started from ca. 220 °C (T_{d5} = 224.1 °C and T_{max} = 251.7 °C) and the weight-loss value was 71.4% after the first-step reaction accompanying the eliminations of camphene and H_2O from the ester groups. The calculated weight-loss values are 65.4 and 69.7% for the quantitative camphene elimination and the subsequent dehydration, respectively, leading to the formation of an acid anhydride moiety as the ideal final product. The observed weight-loss value was larger than the expected one because of the other random decomposition of the polymers, although the anhydride group was partially produced but not all. The decomposition temperature for PIBoA was similar to that for PtBA and much lower than those for PCHA and PBoA, of which the T_{d5} and T_{max} values were over 270 and 340 °C, respectively. When TsOH as the acid was added to the polymers, the T_{d5} values significantly decreased. The olefin elimination from the PIBoA side-chain occurs in a temperature range below 100 °C in the presence of TsOH (5 mol %), similar to the reaction of PtBA. The decomposition of PBoA and PCHA was accelerated by the addition of TsOH, but the weight loss occurred at a higher temperature and the slope of the weight-loss curve was lower.

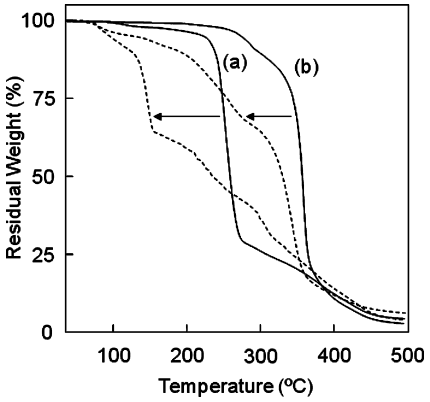

Figure 3. TG curves for (a) PIBoA and (b) PBoA in the absence (solid curves) and presence (dash curves) of TsOH (5 mol %) at the heating rate of 10 °C/min in a nitrogen stream.

In general, the olefin elimination readily occurs for the *tert*-alkyl esters to produce acid products in a quantitative yield, while only partially for the *sec*-alkyl esters, and such deprotection reactions are accelerated in the presence of an acid catalyst.[24,27] The decomposition behavior of the isobornyl ester is similar to that for the *tert*-alkyl esters, and quite different from those for the other secondary alkyl esters including the bornyl ester.[29−31] The high reactivity of the isobornyl ester can be accounted for by the easy elimination of the leaving group at the more favorable conformation, which is fixed by the ring structure of the ester alkyl group. In fact, a broad peak due to the O−H stretching of the carboxylic acid appeared at 2500 to 3600 cm^{-1} and the C═O stretching at 1733 cm^{-1} shifted to the shorter wavenumber region in the IR spectra of the PIBoA films containing 6 mol % of TsOH after heating at 100 °C for 1 h, but the ratio of the decomposition was much lower than the decomposition of PtBA under similar conditions (see Figure S1 in the Supporting Information). The decomposition of the thermally stable PIBoA partly occurred under severe conditions such as the heating at 150 °C for 1 h. The thermal resistance of PIBoA is determined by the bulky and hydrophobic ester, judging from the T_g value being lower than the reaction temperature.

Deprotection of PtBA Using PAG. In this study, the commercially available BCD[37] and NIT[38−40] were used as the PAGs, which are often used as a catalyst for the photoinduced cationic polymerization,[41] UV curing,[42] and photoresist[24,25] processes. The mechanisms for the photodecomposition of BCD and NIT are shown in Schemes 2 and 3, respectively. The UV light irradiation with a short wavelength (less than 300 nm) induces the elimination of N_2 from BCD, resulting in the formation of a carbene compound that further undergoes Wolff rearrangement and provides a sulfonic acid. NIT directly provides the acid by photodecomposition. As described in the literature,[37−40] proton-donating compounds such as water contained in a reaction system participate in the reactions for the acid formation. The results of the TG analysis for the PtBA films containing 5.0 mol % BCD after preirradiation of a UV light for a given time are shown in Figure 4a and Table 1. As a result, the T_{d5} value decreased to 165 °C in the presence of BCD without photoirradiation, and the UV irradiation accelerated the isobutene elimination. The onset temperature of the decomposition depended on the photoirradiation time, i.e., the amount of the sulfonic acid formed during the photoirradiation. The conversion of the BCD decomposition was monitored by IR spectroscopy. A peak due to the C═N stretching of BCD at 2115 cm^{-1} decreased and a broad peak due to the O−H stretching appeared at 2500−3600 cm^{-1} in the

Scheme 2

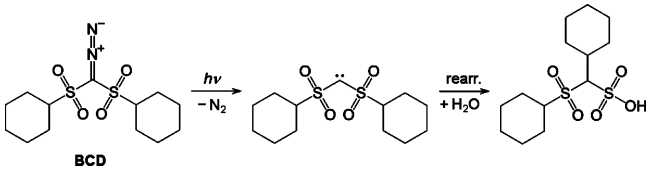

Scheme 3

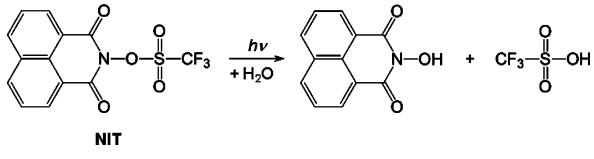

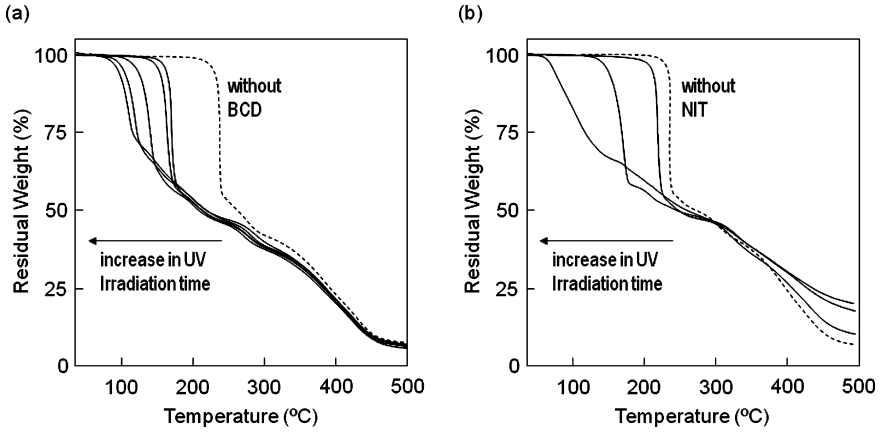

Figure 4. TG curves for PtBA with PAG at the heating rate of 10 °C/min in a nitrogen stream. (a) In the presence of BCD (5.0 mol %) (solid curves) and in the absence of BCD (dash curve). The photoirradiation times, 0, 1, 4, 9, and 16 h. (b) In the presence of NIT (1.0 mol %) (solid curves) and in the absence of NIT (dash curve). The photoirradiation times, 0, 10, and 50 min.

Table 1. Photochemical Acid-Catalyzed Deprotection of PtBA in the Presence of PAG

PAG (mol %)	irradiation time (min)	decomposition ratio (%)	T_{d5} (°C)	T_{max} (°C)	T_{end} (°C)	weight loss (%)	X (%)
none	0	0	232.7	235.0	246.5	46.3	~100
BCD (5.0)	0	0	164.6	173.0	191.4	45.4	~100
	60	12	154.8	167.4	187.4	44.8	~100
	240	53	125.0	144.2	169.1	42.4	96.8
	540	73	106.1	122.7	143.8	34.0	77.7
	960	88	98.5	113.7	133.1	29.9	68.3
NIT (1.0)	0	[a]	210.7	219.2	235.6	47.1	~100
	10	[a]	149.2	172.0	186.3	42.4	96.8
	50	[a]	73.6	105.4	160.3	34.0	77.6

[a]Not determined.

Scheme 4

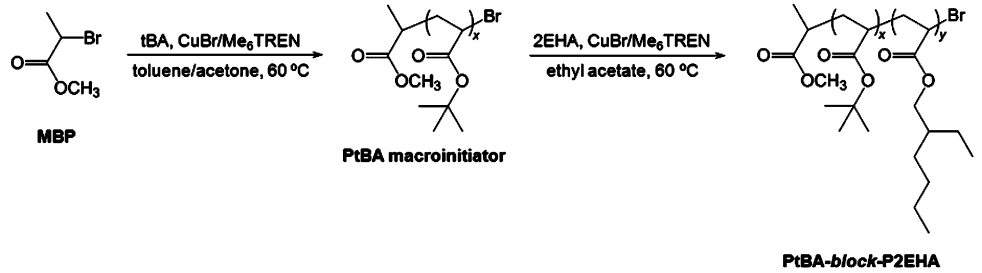

IR spectrum during photoirradiation. As shown in Table 1, almost all of the diazo group decomposed during the 16-h photoirradiation. In contrast to the facile photodecomposition, BCD was thermally stable and no change was detected in the IR spectrum even after heating at 80 °C for 7 h in the dark. Figure 4b shows the results for the TG analysis of PtBA in the presence of NIT. The T_{d5} value decreased from 211 to 149 and 74 °C depending on the amount of the generated trifluoromethane sulfonic acid during the photoirradiation. The NIT more effectively functioned as the PAG with a high sensitivity, and therefore, the reaction conditions such as the small amount of PAG (1 mol % versus the *tert*-butyl group) and short irradiation time (within 1 h) were enough to induce the quantitative acid-catalyzed deprotection of PtBA (Table 1). This facile reaction using NIT under the conditions of 1 mol % content and 50-min irradiation is comparable to the results when using a greater amount of BCD (5 mol %) under a much longer photoirradiation (16 h).

Preparation of Block Copolymers. Block copolymers including both the reactive and the low-T_g polymer segments with a well-defined chain structure were prepared by ATRP.[32] A macroinitiator was first synthesized by the polymerizations of tBA and 2EHA using MBP and BHD as the mono- and difunctional initiators, respectively (Schemes 4–6). The CuBr was used as the catalyst in combination with Me_6TREN in a mixture of toluene and acetone (70/30 wt %) at 60 °C. The PtBA macroinitiators with different molecular weights ($M_{n,NMR}$ = 4.0–12.2 × 10^3) and narrow molecular weight distributions (M_w/M_n = 1.08–1.13) were obtained by changing the polymerization time (i.e., conversion) and the monomer/initiator ratio (see Table S2 in the Supporting Information for the detailed results of the polymerization). The degree of polymerization (DP) was determined by the ratio of the peak intensities due to the methoxy group in the terminal group at the α-chain end and the methine hydrogen of the repeating unit in the chain for PtBA in the ^{1}H NMR spectrum (see Figure S2

Scheme 5

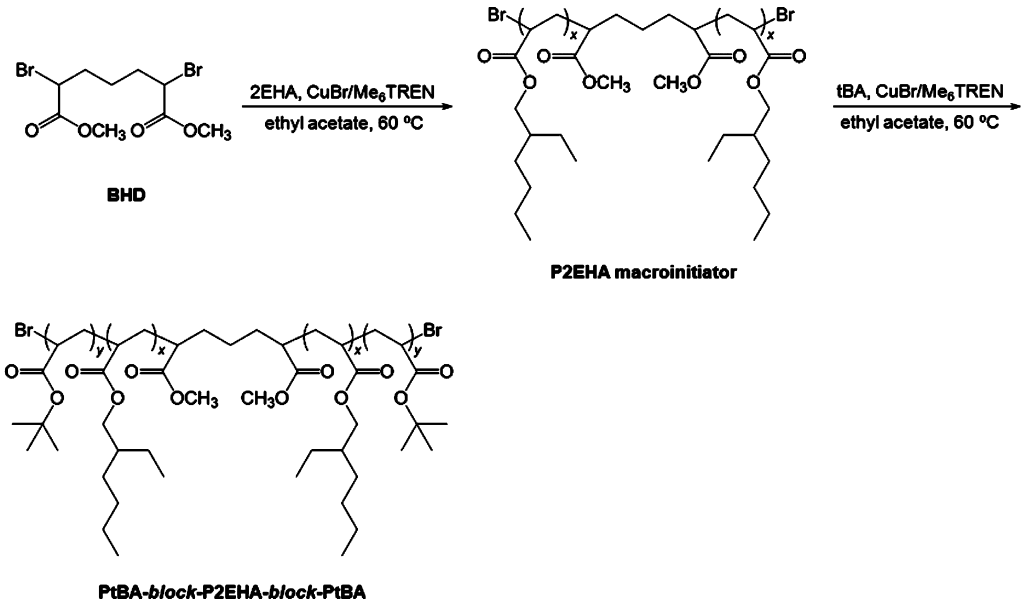

Scheme 6

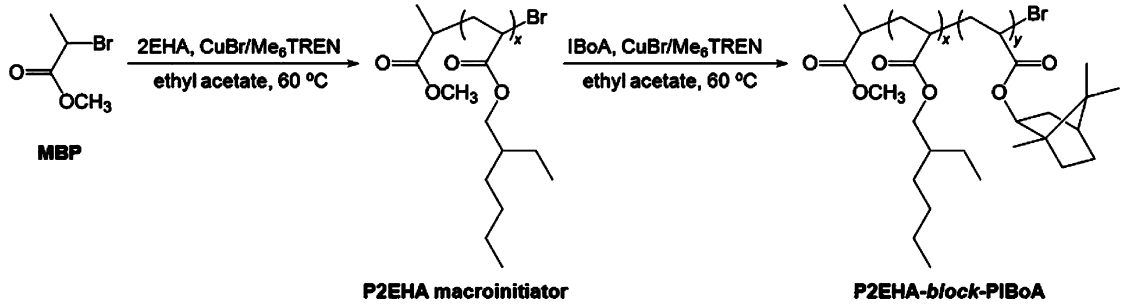

Table 2. Molecular Characteristics and Peel Strength of the PtBA-*block*-P2EHAs in the Presence of TsOH as the Dismantlable Adhesives upon Heating[a]

				peel strength (N/m)	
adhesive	$M_{n,SEC} \times 10^{-3}$	tBA content (mol %)	T_g (°C)	before heating	after heating[b]
$PtBA_{30}$-*block*-$P2EHA_{95}$ (B-1)	18.6	24.0	−69	4.4	1.9
$PtBA_{61}$-*block*-$P2EHA_{68}$ (B-2)	20.0	47.3	−70	3.7	1.4
$PtBA_{61}$-*block*-$P2EHA_{34}$ (B-3)	12.6	64.2		55	
$PtBA_{94}$-*block*-$P2EHA_{50}$ (B-4)	19.5	65.2		310	~0[c]
$PtBA_{94}$-*block*-$P2EHA_{36}$ (B-5)	18.5	72.3	−59, 1	[d]	~0
P(tBA-*co*-2EHA) (random)	19.8	50.0	−42	2.9	2.3
$PtBA_{61}$/$P2EHA_{52}$ (blend)	8.4/8.4	54.0	−75(−58[e])	[f]	

[a]180° peel test using the test specimen of a PET film and a stainless steel plate bonded by PtBA-*block*-P2EHAs as the pressure-sensitive adhesive in the presence of 5 mol % TsOH. Peel rate, 30 mm/min. [b]100 °C for 1 h. [c]After UV irradiation for 8 h and the subsequent heating at 100 °C for 1 h in the presence of BCD (5.0 mol %) (See also Table 3). [d]Not determined because of strong stick−slip failure. [e]See ref 34. [f]Not determined because of a very low strength.

in the Supporting Information). The functionality of the ω-chain end (f) was determined based on the peak intensity due to the CH hydrogen of the terminal tBA unit at the ω-chain end versus the intensity of the characteristic peak at the α-chain end. The f values were greater than 0.9 at the 90% conversion, but they decreased during further polymerization and reached 0.75 at the 98.6% conversion due to the bimolecular termination occurrence. The P2EHA macroinitiators with well-controlled chain structure was similarly synthesized using MBP and BHD as the initiators; $M_{n,NMR}$ = 6.4−10.7 × 10^3 and M_w/M_n = 1.16−1.19 (see Table S2 in the Supporting Information).

The PtBA and P2EHA macroinitiators were used for the subsequent block copolymer synthesis by ATRP using a second monomer (2EHA, tBA, or IBoA) in ethyl acetate at 60 °C. In this study, three kinds of block copolymers, i.e., PtBA-*block*-P2EHA, PtBA-*block*-P2EHA-*block*-PtBA, and P2EHA-*block*-PIBoA were prepared as shown in Schemes 4−6. The SEC peak shifted to the high molecular weight region while maintaining a narrow molecular weight distribution after the

second-step polymerization (see Figure S3 in the Supporting Information). These results indicated that the block copolymers are of a highly controlled molecular weight, distribution, sequence, and chain-end structures (see Table S3 in the Supporting Information).

In the DSC curves of the PtBA-*block*-P2EHAs, the T_g due to the P2EHA segments was observed at −70 to −59 °C, depending on the tBA contents of the block copolymers (Table 2). These values were slightly higher than the T_g value (−75 °C) for the homopolymer of 2EHA. The T_g due to the PtBA segment was observed at 1 °C for $PtBA_{94}$-*block*-$P2EHA_{36}$ (B-5) with a 64.4 wt % tBA content, but no transition was detected for the PtBA segments in the other block copolymers with lower tBA contents. All the T_g values for the P2EHA segments observed in this study were lower than those in the literature.[34] This is due to the low molecular weight. The random copolymer gave a single intermediate T_g at −42 °C, as expected. Microphase separation between the PtBA and P2EHA segments of the block copolymers was directly confirmed by AFM observation. Figure 5 shows the height

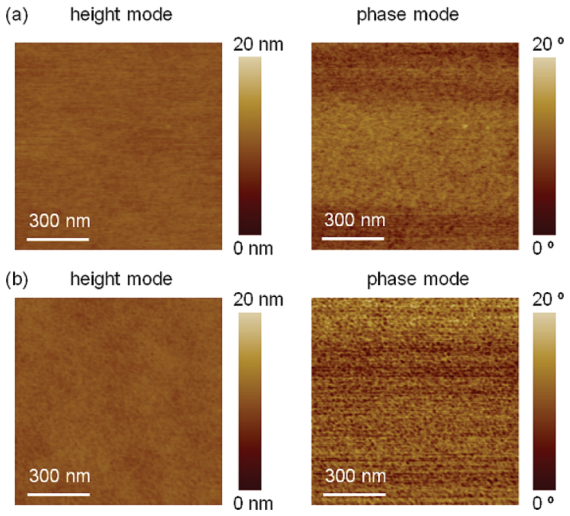

Figure 5. AFM images of the adhesive polymer film surface ($PtBA_{94}$-*block*-$P2EHA_{36}$, B-5, NIT 0.2 mol %) in height and phase modes. (a) Before and (b) after UV irradiation for 1 h and postbalking at 100 °C for 1 h. Observation area 1 μm × 1 μm.

and phase images for the block copolymer including NIT as the PAG before and after the UV irradiation and postbaking. This indicates that the polymer has a flat and microphase-separated structure based on the height and phase images, respectively. The microphase separation was more clearly observed after the UV and heat treatment because of the formation of the hydrophilic and high-T_g PAA domain.

180° Peel Test. The adhesion strength was investigated using the test specimen of a PET film and a stainless steel plate as the substrates and the acrylate block copolymers as the pressure-sensitive adhesive. The PET film with a 20-mm width was peeled at the rate of 30 mm/min. This peel rate is one-tenth of the standard rate described in ASTM and JIS, due to avoidance of stick−slip failure based on the sticky adhesive properties of the used materials. The cohesive force of the adhesives sensitively depended on the copolymer composition, as shown in the peel strength of the adhesives in Table 2; The peel strength of the PtBA-*block*-P2EHA increased to 310 N/m when the tBA content was 65 mol % (B-4). The stick−slip failure was observed even under the conditions using the low peeling rate for the PtBA-*block*-P2EHA with a higher tBA content (B-5). The T_g value of the PtBA segments is higher than those for the conventional pressure-sensitive adhesives, and therefore, stick−slip failure tends to readily occur. In general, peel strength significantly depends on a peel rate when the cohesive failure is dominant. The peel rate dependence was checked for several block copolymers in the present study; The polymer with the large amount of the high-T_g PtBA and PIBoA segments led to stick−slip failure even at a low peel rate, while the polymers containing the large amount of the low-T_g P2EHA segment showed no stick−slip behavior and the peel strength significantly depended on the peel rate. For example, the peel strength values increased to 100 and 190 N/m at the peel rates of 200 and 300 mm/min, respectively, during the peel strength measurement using poly($2EHA_{57}$-*block*-$PIBoA_{29}$). For most of the adhesive polymers used in this study, cohesive failure was predominant because of the weak intermolecular interactions between the polymer chains with a relatively low molecular weight and the nonpolar ester groups in the side chain.

We investigated the change in the peel strength after heating in order to evaluate the properties of the polymers as the dismantlable adhesives in the presence of TsOH. As a result, a greater decrease was observed in the strength for the adhesives using the block copolymers than when using a random copolymer (Table 2). This suggests that the phase-separated polymer structure of the adhesives plays a role in the change of the adhesion properties during the debonding process, i.e., the block copolymer structure has superior dismantlable adhesion properties due to greater changes in the polymer morphology and surface structures of the adherent. The blend of PtBA and P2EHA showed only poor characteristics as adhesives, providing too low a peel strength to be determined under these conditions. We also examined the adhesion property of two types of blends of the block and homopolymers, PtBA-*block*-P2EHA/PtBA and the PtBA-*block*-P2EHA/P2EHA containing the 60−70 mol % of the total P2EHA segment, but they showed very low peel strength and insensitive response to heating for dismantling. The blend with a lower P2EHA content was not tacky and could not be tested as the adhesive, being different from the favorable results for the block copolymers with a similar composition. This result supports the superiority of the use of block copolymers over polymer blends.

Table 3 summarizes the results for the dual-locked dismantlable adhesion tests using various block copolymers by combination with BCD or NIT. The typical peel strength-displacement curves are shown in Figure 6. No change was observed in the peel strength after heating at 100 °C without any photoirradiation, but the UV irradiation reduced the peel strength to one-fifth of the original strength in the presence of BCD due to the evolution of N_2 gas (Scheme 2). During either heating or irradiation process, no change in the polymer chemical structure occurred, as shown in the NMR spectra of the adhesive polymers recovered after heating at 100 °C for 1 h or photoirradiation for 8 h (Figure 7). In contrast, the adhesive properties of the polymers completely disappeared after the UV irradiation and the postbaking, and the PET films spontaneously peeled off the stainless steel plate. The changes in the polymer solubility and the NMR and IR spectra revealed the quantitative hydrolysis of the block copolymers after treatment with dual external stimuli, i.e., the UV irradiation and the

Table 3. Peel Strength of the PtBA-*block*-P2EHAs, PtBA-*block*-P2EHA-*block*-PtBA, and P2EHA-*block*-PIBoA as the Dual-Locked Dismantlable Adhesives Using BCD or NIT as the PAG[a]

polymer	PAG (mol %)	stimuli: UV	stimuli: heating	peel strength (N/m)
$PtBA_{94}$-*block*-$P2EHA_{50}$	BCD	none	none	310 ± 50
(B-4, tBA content 65.2 mol %)	(5.0)	none	100 °C, 1 h	250 + 45
		8 h	none	60 + 20
		8 h	100 °C, 1 h	~0
$PtBA_{27}$-*block*-$P2EHA_{33}$-*block*-$PtBA_{27}$	NIT	none	none	53 + 2
(B-6, tBA content 62.1 mol %)	(0.2)	none	100 °C, 1 h	61 + 14
		1 h	none	75 + 10
		1 h	100 °C, 1 h	~0
$P2EHA_{57}$-*block*-$PIBoA_{29}$	NIT	none	none	14.4[b]
(B-7, IBoA content 33.7 mol %)	(0.2)	none	150 °C, 1 h	8.5[b]
		1 h	none	20.3[b]
		1 h	150 °C, 1 h	5.7[b]
$P2EHA_{57}$-*block*-$PIBoA_{29}$	NIT	none	none	17 + 3
(B-7, IBoA content 33.7 mol %)	(0.5)	none	150 °C, 1 h	11 + 3
		1 h	none	17 + 2
		1 h	150 °C, 1 h	~0

[a]Peel rate, 30 mm/min. [b]Single measurement.

postbaking. When NIT was used as the PAG, both an improved tolerance to each single stimulus and easy debonding by the sequential dual stimuli were satisfied. No damage was observed in the adhesive qualities during the heating for 1 h, or UV irradiation for 1 h, but spontaneous dismantling was realized by the combination of the dual stimuli of heating and irradiation (Figure 6b). A quicker dismantling was possible with less than 10 min irradiation and heating, although the peel strength was not zero and some adhesive force remained. A high-temperature dismantlable adhesion system was also proposed using P2EHA-*block*-PIBoA as the adhesives. The PIBoA segments showed much better heat resistance than the PtBA segments; The P2EHA-*block*-PIBoAs showed no change in their chemical structure and properties even after heating at 150 °C for 1 h. A higher temperature and greater amount of NIT were needed for the complete dismantling when P2EHA-*block*-PIBoA was used (Table 3). This result indicates that a balance between the tolerance and sensitivity can be changed by the combination of the protected ester groups (*tert*-butyl or isobornyl ester) and the PAG (BCD or NIT, and their amount contained in the polymers).

CONCLUSIONS

We have proposed the new concept of a dual-locked dismantlable adhesion system in which the side-chain ester groups of the adhesive polymers are deprotected due to the dual external stimuli consisting of photoirradiation and postbaking by the action of PAG, leading to a drastic change in the adhesive properties. It was revealed that the well-defined block copolymers consisting of PtBA and PIBoA as the reactive

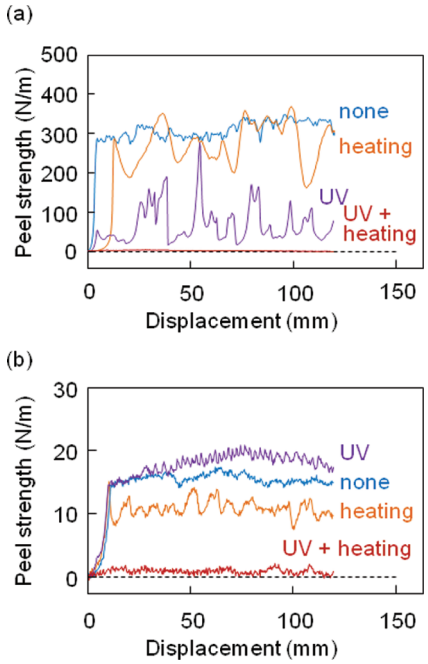

Figure 6. Peel strength-displacement curves during the 180° peel test using the test specimen of a PET film and a stainless steel plate bonded by (a) $PtBA_{94}$-*block*-$P2EHA_{50}$ (B-4) in the presence of 5.0 mol % BCD and (b) P2HEA-*block*-PIBoA (B-7) in the presence of 0.5 mol % NIT. (blue) before UV irradiation and heating, (orange) after heating, (purple) after UV irradiation, and (red) after UV irradiation and the postbake. See Table 3 for the detailed conditions for dismantling.

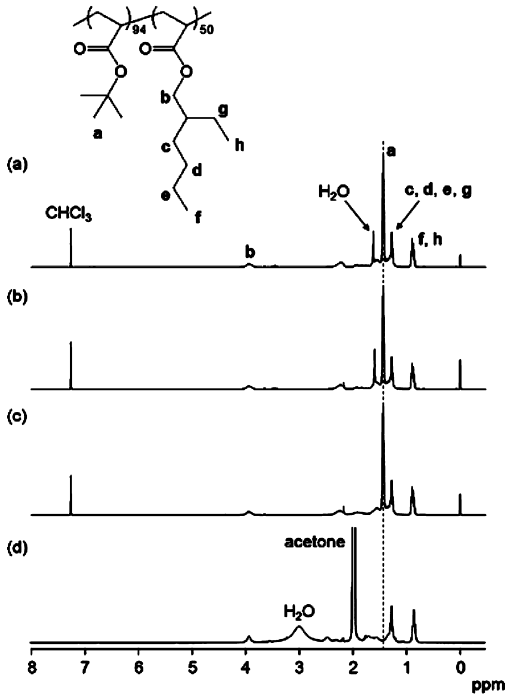

Figure 7. ^1H NMR spectra of the adhesive polymer (B-4) including 5.0 mol % BCD as the PAG before and after any treatment by external stimuli. (a) Before UV irradiation and heating, (b) after heating at 100 °C for 1 h, (c) after UV irradiation at room temperature for 8 h, and (d) after UV irradiation at room temperature for 8 h and the postbaking at 100 °C for 1 h. The spectra shown in a–c were recorded in $CDCl_3$, and d in acetone-d_6 at room temperature.

dx.doi.org/10.1021/am300103c | ACS Appl. Mater. Interfaces 2012, 4, 2124–2132

segment and the P2EHA as the low-T_g segment prepared by ATRP showed excellent dismantling properties due to their phase-separated microstructures. In this study, we demonstrated that the dual-stimuli system is indispensable for achieving both tolerance to an external stimulus for the stability during use and reliable response to stimuli for the on-demand dismantling. We are now continuing the further modification of this dual-locked dismantlable adhesion system for a quicker dismantling and investigating the dynamic properties of the adhesive polymers and the failure mechanism, i.e., the cohesive and interfacial failures.

■ ASSOCIATED CONTENT

Supporting Information

IR and NMR spectra, SEC curves, TG data, and polymerization results (PDF). This material is available free of charge via the Internet at http://pubs.acs.org.

■ AUTHOR INFORMATION

Corresponding Author

*E-mail: sato@a-chem.eng.osaka-cu.ac.jp (E.S.); matsumoto@a-chem.eng.osaka-cu.ac.jp (A.M.).

Notes

The authors declare no competing financial interest.

■ REFERENCES

(1) Cantor, A. *Encyclopedia of Polymer Science and Technology*, 3rd ed.; Kroschwitz, J. I., Ed.; Wiley-Interscience: New York, 2003; Vol. *4*, pp 72−93.
(2) Wang, L. J.; Li, H. Y.; Wong, C. P. *J. Polym. Sci., Part A: Polym. Chem.* **2000**, *38*, 3771−3782.
(3) Chen, J. -S.; Ober, C. K.; Poliks, M. D. *Polymer* **2002**, *43*, 131−139.
(4) Baldan, A. *J. Mater. Sci.* **2004**, *39*, 1−49.
(5) Li, H. Y.; Wong, C. P. *IEEE Trans. Adv. Packag.* **2004**, *27*, 165−172.
(6) Caruso, M. M.; Davis, D. A.; Shen, Q.; Odom, S. A.; Sottos, N. R.; White, S. R.; Moore, J. S. *Chem. Rev.* **2009**, *109*, 5755−5798.
(7) González, L.; Ferrando, F.; Ramis, X.; Salla, J. M.; Mantecón, A.; Serra, A. *Prog. Org. Coat.* **2009**, *65*, 175−181.
(8) Hutchinson, A. R.; Winfield, P. H.; McCurdy, R. H. *Adv. Eng. Mater.* **2010**, *12*, 646−652.
(9) Esser-Kahn, A. P.; Odom, S. A.; Sottos, N. R.; White, S. R.; Moore, J. S. *Macromolecules* **2011**, *44*, 5539−5553.
(10) Yang, S.; Chen, J. -S.; Körner, H.; Breiner, T.; Ober, C. K. *Chem. Mater.* **1998**, *10*, 1475−1482.
(11) Ogino, K.; Chen, J. -S.; Ober, C. K. *Chem. Mater.* **1998**, *10*, 3833−3838.
(12) Malik, J.; Clarson, S. J. *Int. J. Adhes. Adhes.* **2002**, *22*, 283−289.
(13) Nishiyama, Y.; Uto, N.; Sato, C.; Sakurai, H. *Int. J. Adhes. Adhes.* **2003**, *23*, 377−382.
(14) Ishikawa, H.; Seto, K.; Shimotuma, S.; Kishi, N.; Sato, C. *Int. J. Adhes. Adhes.* **2005**, *25*, 193−199.
(15) Shirai, M. *Prog. Org. Coat.* **2007**, *58*, 158−165.
(16) Sekine, T.; Tomita, H.; Obata, S.; Saito, Y. *Electr. Eng. Jpn.* **2009**, *168*, 32−39.
(17) Gilbert, M. D. United States Patent U.S. 7 332 218, February 19, 2008.
(18) Kihara, N.; Ii, R.; Ogawa, A. *J. Polym. Sci., Part A: Polym. Chem.* **2007**, *45*, 963−967.
(19) Sato, E.; Tamura, H.; Matsumoto, A. *ACS Appl. Mater. Interfaces* **2010**, *2*, 2594−2601.
(20) Mukundan, T.; Kishore, K. *Prog. Polym. Sci.* **1990**, *15*, 475−505.
(21) Matsumoto, A.; Higashi, H. *Macromolecules* **2000**, *33*, 1651−1655.
(22) Hatakenaka, H.; Takahashi, Y.; Matsumoto, A. *Polym. J.* **2003**, *35*, 640−651.
(23) Sato, E.; Matsumoto, A. *Chem. Rec.* **2009**, *9*, 247−257.
(24) Ito, H. *Adv. Polym. Sci.* **2005**, *172*, 37−245.
(25) Ito, H.; Willson, C. G. *Polym. Eng. Sci.* **1983**, *23*, 1012−1018.
(26) Schaefgen, J. R.; Sarasohn, I. M. *J. Polym. Sci.* **1962**, *58*, 1049−1061.
(27) Otsu, T.; Yasuhara, T.; Shiraishi, K.; Mori, S. *Polym. Bull.* **1984**, *12*, 449−456.
(28) Otsu, T.; Tatsumi, A.; Matsumoto, A. *J. Polym. Sci., Part C: Polym. Lett.* **1986**, *24*, 113−117.
(29) Imoto, M.; Ito, T.; Otsu, T.; Tsuda, K. *J. Polym. Sci., Part A* **1964**, *2*, 1407−1419.
(30) Ors, J. A.; La Perriere, D. M. *Polymer* **1986**, *27*, 1999−3003.
(31) Matsumoto, A.; Mizuta, K.; Otsu, T. *J. Polym. Sci., Part A: Polym. Chem.* **1993**, *31*, 2531−2539.
(32) Queffelec, J.; Gaynor, S. G.; Matyjaszewski, K. *Macromolecules* **2000**, *33*, 8629−8639.
(33) Vidts, K. R. M.; Dervaux, B.; Du Prez, F. E. *Polymer* **2006**, *47*, 6028−6037.
(34) Penzel, E.; Rieger, J.; Schneider, H. A. *Polymer* **1997**, *38*, 325−337.
(35) Shetter, J. A. *J. Polym. Sci., Part B: Polym. Lett.* **1963**, *B1*, 209−213.
(36) Eisenberg, A.; Yokoyama, T.; Sambalido, E. *J. Polym. Sci., Part A-1* **1969**, *7*, 1717−1728.
(37) Sander, W.; Strehl, A.; Winkler, M. *Eur. J. Org. Chem.* **2001**, 3771−3778.
(38) Ortica, F.; Scaiano, J. C.; Pohlers, G.; Cameron, J. F.; Zampini, A. *Chem. Mater.* **2000**, *12*, 414−420.
(39) Okamura, H.; Sakai, K.; Tsunooka, M.; Shirai, M.; Fujiki, T.; Kawasaki, S.; Yamada, M. *J. Photopolym. Sci. Technol.* **2003**, *16*, 87−90.
(40) Malval, J. -P.; Suzuki, S.; Morlet-Savary, F.; Allomas, X.; Fonassier, J. −P.; Takahara, S.; Yamaoka, T. *J. Phys. Chem. A* **2008**, *112*, 3879−3885.
(41) Park, J.; Kihara, N.; Ikeda, T.; Endo, T. *Macromolecules* **1997**, *30*, 3414−3416.
(42) Shirai, M.; Morishita, S.; Okamura, H.; Tsunooka, M. *Chem. Mater.* **2002**, *14*, 334−340.